

Artificial Hawking Radiation in Non-Hermitian Parity-Time Symmetric Systems

Marcus Stålhammar¹, Jorge Larana-Aragon¹, Lukas Rødland¹, and Flore K. Kunst²

¹*Department of Physics, Stockholm University, AlbaNova University Center, 106 91 Stockholm, Sweden and*

²*Max-Planck-Institut für Quantenoptik, Hans-Kopfermann-Straße 1, 85748 Garching, Germany*

We show that the exceptional surfaces of linear three-dimensional non-Hermitian parity-time-symmetric two-band models attain the form of topologically stable tilted exceptional cones. By relating the exceptional cones to the eigenvalues of Dirac operators, we find a connection between the exceptional cone and the light cone of an observer in the vicinity of a Schwarzschild black hole. When the cone overtilts, light-like particle-antiparticle pairs are created resembling Hawking radiation. We also investigate dissipative features of the non-Hermitian Hamiltonian related to the latter and comment on potential realizations in laboratory setups.

I. INTRODUCTION

Since the experimental discovery of the quantum Hall effect in the 1980s [1], topology has played a prominent role in condensed matter physics. A large part of the studies during the last decades have been devoted to gapped topological insulators [2, 3] and gapless semimetals, such as graphene [4] and Weyl semimetals (WSMs) [5], whose Bloch bands are characterized by distinct topological invariants [6]. The progress in the latter led to the realization of the elusive Weyl fermions which, despite evading discovery for nearly a century after being theoretically predicted in the context of particle physics [7], were realized as quasi-particles near the point-like band crossings in WSMs [8–10]. This led to further observations of theoretical concepts known from high-energy physics, such as the chiral anomaly, which found its analogue experimental quantity in WSMs [11–14].

The general idea of analogues between different areas of physics is especially relevant in the context of quantum gravity and black holes. Even though black holes have provided key insights into the fundamental nature of spacetime, direct experimental input is difficult to obtain. However, through investigations in analogue models, quantum gravity can be studied in laboratory setups [15, 16]. In this context, the aforementioned WSMs have received great attention due to the behavior of their cone-like dispersion, called the Weyl cone. In particular, the tilting of the Weyl cone resembles the behavior of spacetime light cones [17]. This intuition is formalized via the construction of a rigorous relation between the transition from type I to type II WSMs, as the Weyl cone overtilts, and the tilting of an observer’s light cone when crossing the black hole horizon in the infalling coordinate frame [18, 19]. With this as starting point, recent studies [20–24] have focused on investigating potential analogues of Hawking radiation. As Hawking pointed out and despite the classical intuition, black holes emit thermal radiation at a characteristic temperature upon evaporating when taking quantum effects into account [25].

Intuitively, the emission of thermal radiation can be associated with loss of energy from a system to its environment. This suggests that Hermitian systems might not be the most optimal candidates for a direct analogy with such dissipative features. On the other hand, many recent studies of topological phases have focused on non-Hermitian (NH) Hamiltonians, which serve as an effective description of systems subject

to gain and loss [26]. Naturally, these Hamiltonians are fundamentally different from their Hermitian counterparts, the most prominent distinction being complex eigenvalues and separate sets of left and right eigenvectors. Furthermore, the nodal structures of NH systems consist of exceptional points (EPs) at which not only the eigenvalues, but also the eigenvectors coalesce [27]. The sets of EPs exhibit fascinating topological properties [28–36], which can be investigated in experimental simulations at remarkable precision [37]. In particular, NH systems find high experimental relevance in optics, where they effectively describe photonic systems subject to parity-time (\mathcal{PT}) symmetry [38, 39]. \mathcal{PT} -symmetric systems host separate regions with real and complex eigenvalues which are separated by EPs, where \mathcal{PT} -symmetry is spontaneously broken. Consequently, these regions are called the \mathcal{PT} -unbroken phase and the \mathcal{PT} -broken phase respectively.

Motivated by the natural inclusion of dissipative effects and the high experimental relevance of NH \mathcal{PT} -symmetric systems, we in this work construct an analogy between the latter and black holes. We find that the set of EPs of such systems linear in momentum constitute a tilted cone, which we refer to as the exceptional cone (EC). We extend the analogy between Weyl cones and light cones to include ECs. This allows us to relate the EC to an observer’s light cone in the vicinity of a stationary 4D Schwarzschild black hole. By using this analogue system, we calculate the leading order contribution to Hawking radiation. Additionally, we interpret the result in terms of dissipative features unique to NH systems. We conclude by investigating the latter in a tight-binding model, whose low-momentum description coincides with the initial NH system.

Throughout this article, we are working in natural units where $\hbar = c = k_B = G_N = 1$.

II. NODAL TOPOLOGY IN TWO-BAND MODELS

A non-interacting Hermitian two-band model in its most general form is given by the following Bloch Hamiltonian in reciprocal space

$$H(\mathbf{k}) = d_0(\mathbf{k})\sigma^0 + \mathbf{d}(\mathbf{k}) \cdot \boldsymbol{\sigma}, \quad (1)$$

where \mathbf{k} is the lattice momentum in the appropriate dimension, σ^0 is the 2×2 identity matrix, $\boldsymbol{\sigma} = (\sigma^x, \sigma^y, \sigma^z)$ are the Pauli matrices, $\mathbf{d}(\mathbf{k}) = [d_x(\mathbf{k}), d_y(\mathbf{k}), d_z(\mathbf{k})]$, and d_μ are continuously differentiable real-valued functions of \mathbf{k} for

$\mu = 0, x, y, z$. From here, we use the notation $d_\mu(\mathbf{k}) =: d_\mu$ for simplicity, restoring the \mathbf{k} -dependence when appropriate. The corresponding energy eigenvalues are

$$E_\pm = d_0 \pm \sqrt{d_x^2 + d_y^2 + d_z^2}, \quad (2)$$

and the nodal points are given by the intersections of the eigenvalues, which arise from solutions to

$$\sqrt{d_x^2 + d_y^2 + d_z^2} = 0. \quad (3)$$

Nodal points are generically of codimension 3, meaning that they occur in $D = 3$ or higher. There are, however, several ways of reducing the codimension of the nodal structures. The most obvious is if the system of equations in Eq. (3) is underdetermined, but such a case is often not stable and thus relies on fine-tuning. Another option is to impose certain symmetries on the system. One such which finds wide applications in both condensed matter physics as well as optics, is \mathcal{PT} symmetry. Let us, for the sake of illustration, investigate how \mathcal{PT} symmetry affects the codimension of the set of nodal points. Following Refs. 40 and 41, we represent \mathcal{P} symmetry by a \mathcal{P} -matrix, and \mathcal{T} symmetry by a \mathcal{K} -matrix, where $\mathcal{K}\mathcal{K}^* = \pm\mathbb{I}$, $\mathcal{P}^2 = \mathbb{I}$ and $\mathcal{K}\mathcal{P}^* = \pm\mathcal{P}\mathcal{K}$. We focus on the symmetry class where $\mathcal{K}\mathcal{K}^* = \mathbb{I}$ and $\mathcal{K}\mathcal{P}^* = \mathcal{P}\mathcal{K}$, and choose the following representation:

$$\mathcal{P} = \sigma^y, \quad \mathcal{K} = \sigma^z. \quad (4)$$

Imposing \mathcal{PT} symmetry on a generic two-band Hamiltonian, i.e., in Eq. (1),

$$H_{\mathcal{PT}} = \mathcal{P}\mathcal{K}H_{\mathcal{PT}}^*(\mathcal{P}\mathcal{K})^{-1}, \quad (5)$$

implies that $d_0, d_x, d_y \in \mathbb{R}$ and $d_z = 0$. Since $d_z = 0$ is satisfied for all \mathbf{k} as a consequence of the symmetry, the nodal structure is determined by a system of merely two equations. Therefore, \mathcal{PT} -symmetric 2D systems generically host topologically stable nodal points, while 3D systems host nodal lines [42–47].

So far, we have restricted the discussion to Hermitian systems. However, in recent years, many studies of NH Hamiltonians have been conducted [26]. The mathematical description of systems with such an effective description is similar to the above reasoning, and in its most general form, a non-interacting, NH two-band system is given by

$$H = d_0\sigma^0 + \mathbf{d} \cdot \boldsymbol{\sigma}, \quad (6)$$

where now d_μ denote *complex valued* continuously differentiable functions of the lattice momentum \mathbf{k} . Decomposing $\mathbf{d} = \mathbf{d}_R + i\mathbf{d}_I$, the corresponding complex eigenvalues are

$$E_\pm = d_0 \pm \sqrt{d_R^2 - d_I^2 + 2id_R \cdot \mathbf{d}_I}. \quad (7)$$

Hence, the nodal structure is given by the following system of equations,

$$d_R^2 - d_I^2 = 0, \quad \mathbf{d}_R \cdot \mathbf{d}_I = 0. \quad (8)$$

At this point we set $d_0 = 0$, since we study the topology of the nodal structure, which is not affected by d_0 . In contrast to the eigenvalue degeneracies in Hermitian systems, the nodal points in NH systems are *exceptional* (except for when $|\mathbf{d}| = 0$), meaning that not only the eigenvalues, but also the eigenstates coalesce [27]. Also, the exceptional nodal structure is determined by the simultaneous solution of two equations, meaning that stable EPs occur already in 2D systems, while in 3D, they attain the form of closed lines [26]. As in the case of Hermitian systems, the codimension of exceptional nodal structures can be decreased by imposing symmetries, e.g., \mathcal{PT} symmetry. In a NH setup, the constraint (5) reduce to the following:

$$H_{\mathcal{PT}} = d_x\sigma^x + d_y\sigma^y + id_z\sigma^z, \quad (9)$$

with $d_x, d_y, d_z \in \mathbb{R}$. The corresponding eigenvalues are then

$$E_{\pm, \mathcal{PT}} = \pm \sqrt{d_x^2 + d_y^2 - d_z^2}. \quad (10)$$

The EPs are defined by only one equation, and therefore stable EPs protected by \mathcal{PT} symmetry occur already in 1D systems, exceptional lines in 2D and exceptional surfaces in 3D [36]. Furthermore, the EPs separates the eigenvalue spectrum into two different phases: the \mathcal{PT} -unbroken phase where the eigenvalues are purely real, and the \mathcal{PT} -broken phase where they are purely imaginary.

III. CONES IN BAND STRUCTURES AND LIGHT CONES

Here, we briefly review the method relating the dispersion of a Dirac operator to a field theory in curved spacetime. We refer the interested reader to Refs. 18 and 19 for a more thorough treatment. Inspired by this, we also extend this relation to include NH systems by relating the ECs arising in \mathcal{PT} -symmetric systems to light cones.

A. Dirac-like Operators and Black Holes

Recent works has shown that tilted WSMs can be related to gravitational light cones [20–24]. The starting point of this analogy is the Weyl Hamiltonian

$$H = \boldsymbol{\kappa} \cdot \mathbf{k}\sigma^0 + \mathbf{k} \cdot \boldsymbol{\sigma}, \quad (11)$$

where $\boldsymbol{\kappa} \in \mathbb{R}^3$ is the tilting parameter and $\mathbf{k} := (k_x, k_y, k_z)$. The corresponding energy eigenvalues read

$$E_\pm = \boldsymbol{\kappa} \cdot \mathbf{k} \pm \sqrt{k_x^2 + k_y^2 + k_z^2}. \quad (12)$$

and constitutes a cone in energy-momentum space tilted by $\boldsymbol{\kappa}$, which is displayed in Fig. 1. $|\boldsymbol{\kappa}| < 1$ and $|\boldsymbol{\kappa}| > 1$ corresponds to type I and type II WSMs respectively. The transition between the different types, i.e., when the cone overtilts, is intuitively similar to the titling of a light cone when the corresponding observer crosses the horizon of a Schwarzschild

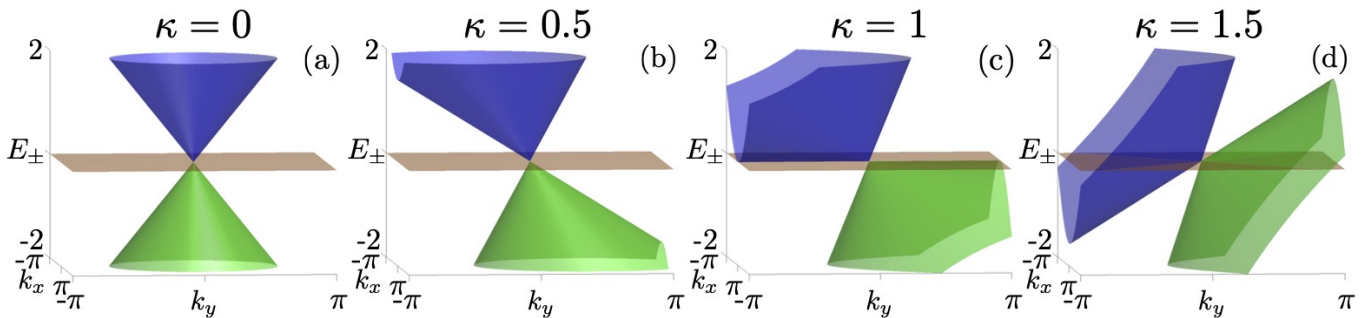


Figure 1. Illustration of the eigenvalues corresponding to Eq. (11) for $\kappa = (\kappa, 0, 0)$ in the plane $k_z = 0$ for different values of κ . When $\kappa > 1$, the cone overtilts in analogy to a light cone when the corresponding observer crosses the horizon of a Schwarzschild black hole. Thus, the two phases type I ($\kappa < 1$) and type II ($\kappa > 1$) intuitively resemble the exterior and the interior of a black hole respectively.

black hole. This intuition is made formal by relating the Hamiltonian Eq. (11) to the metric of a curved spacetime. This is in fact possible for any Dirac-like operator, and we refer to Refs. 18 and 19 for a complete and detailed treatment. The key is the so-called *vielbeins* e^μ_α and their inverses e_μ^α , which in general relativity are used to define local patches of orthonormal coordinate systems in spacetime [48]. They relate to the spacetime metric as $g_{\mu\nu} = e_\mu^\alpha e_\nu^\beta \eta_{\alpha\beta}$, with $\eta_{\alpha\beta} = \text{diag}(-1, 1, 1, 1)$. Following Refs. 18 and 19, the Hamiltonian Eq. (11) can be put on the form

$$H = e^i_a k_i \sigma^a + e^i_0 k_i \sigma^0 \quad (13)$$

with $i, a = x, y, z$, $e^i_a = 1$, $e^i_0 = \kappa^i$ and $e^0_0 = 1$ [18, 19]. The line element of the corresponding analogue spacetime metric then reads

$$ds^2 = -\left(1 - |\kappa|^2\right) dt^2 + |d\mathbf{x}|^2 + 2\kappa \cdot d\mathbf{x} dt, \quad (14)$$

where $d\mathbf{x} = (dx, dy, dz)$ and $|d\mathbf{x}|^2 = dx^2 + dy^2 + dz^2$. Eq. (14) describes an event horizon at $|\kappa| = 1$, which coincides exactly with when the Weyl cone overtilts, cf. Fig. 1.

As previously indicated, an intriguing feature of black holes is that they evaporate away over time. A natural question to ask is whether or not the resulting artificial event horizon in the analogue model is emitting radiation. If that is the case, the question would be if it can be related to a physical quantity that can be measured in a laboratory setup. Interestingly enough, this is something that seems to divide the community. On the one hand, there are works claiming that artificial spontaneous Hawking radiation is present in WSMs [20, 22], while other works claim that there is no radiative process [24]. As we already mentioned, NH systems seem better suited to describe these type of phenomena, due to their dissipative features, e.g., gain and loss [26]. Motivated by the latter, we below present an extension of the analogy between Weyl cones and light cones to NH systems.

B. NH Systems and Curved Spacetime

The relation between Dirac operators and spacetime metrics cannot be naively extended to NH operators. Also, since

the eigenvalues of such operators are complex, there is no clear intuitive picture to follow, as in the case of the Weyl Hamiltonian. However, by considering the eigenvalues of a NH \mathcal{PT} -symmetric Hamiltonian,

$$H_{\mathcal{PT}} = d_x \sigma^x + d_y \sigma^y + i d_z \sigma^z, \quad (15)$$

$$E_{\pm, \mathcal{PT}} = \pm \sqrt{d_x^2 + d_y^2 - d_z^2}, \quad (16)$$

and investigating the EPs of such systems, interesting observation can be made. Explicitly, the EPs are determined by

$$d_z = \pm \sqrt{d_x^2 + d_y^2}, \quad (17)$$

which is on the same form as the eigenvalues of a Hermitian Dirac operator. A consequence of this, is that the EPs of \mathcal{PT} -symmetric NH Hamiltonians linear in momentum form a (possibly tilted) cone, a proof of which we provide in Appendix A. This suggests that the intuitive light cone analogue in NH systems is not the eigenvalues themselves, but rather the EPs, a relation/an analogy we now formalize.

Consider the NH \mathcal{PT} -symmetric two-band model

$$H = k_x \sigma^x + k_y \sigma^y + i(k_z - \kappa k_x) \sigma^z. \quad (18)$$

with its corresponding eigenvalues

$$E_{\pm} = \pm \sqrt{k_x^2 + k_y^2 - (k_z - \kappa k_x)^2} \quad (19)$$

The EPs are explicitly given by,

$$k_z = \kappa k_x \pm \sqrt{k_x^2 + k_y^2}. \quad (20)$$

The latter constitutes a cone of EPs in momentum space tilted in the k_x -direction by the parameter κ , which we refer to as the *exceptional cone* (EC) in what follows. Note that when $(k_z - \kappa k_x)^2 < k_x^2 + k_y^2$ (momenta outside the EC), the eigenvalues are purely real and the system is in the \mathcal{PT} -unbroken phase, while $(k_z - \kappa k_x)^2 > k_x^2 + k_y^2$ (momenta inside the EC) results in purely imaginary eigenvalues, leaving the system in the \mathcal{PT} -broken phase. These phases are separated by the EC, where \mathcal{PT} symmetry is spontaneously broken. Similar to the Weyl cones, the EC overtilts when $|\kappa| > 1$. Notably, k_z takes

the same form as the eigenvalues of a Dirac-like operator, for instance on the form,

$$\hat{k}_z = \kappa k_x \sigma^0 + k_x \sigma^x + k_y \sigma^y. \quad (21)$$

This operator, and other Dirac-like operators obtained this method, necessarily are \mathcal{PT} -symmetric as well. Adding a \mathcal{PT} symmetry breaking term to Eq. (21), and following the procedure backwards, results in a NH Hamiltonian that is no longer \mathcal{PT} -symmetric, which contradicts the initial assumptions. This is shown to hold for more general operators in Appendix A. Hence, the eigenvalues of \hat{k}_z constitute a topologically stable cone protected by \mathcal{PT} symmetry.

The connection between the EC and the eigenvalues of a Dirac-like operator, such as \hat{k}_z , allows us to further relate the EC to a gravitational light cone. Recalling Sec. III A, \hat{k}_z can be associated to a spacetime metric via the vielbein formalism,

$$\hat{k}_z = e^i_a k_i \sigma^a + e^i_0 k_i \sigma^0, \quad (22)$$

with $i, a = x, y$, $e^i_a = 1$, $e^i_0 = \kappa$ and $e^0_0 = 1$. In Appendix A, we again provide an argument valid for more general systems. The analogue curved spacetime metric is given by $g_{\mu\nu} = e_\mu^\alpha e_\nu^\beta \eta_{\alpha\beta}$, and the corresponding line element $ds^2 = g_{\mu\nu} dx^\mu dx^\nu$ reads,

$$ds^2 = - (1 - \kappa^2) dt^2 + dx^2 + dy^2 + 2\kappa dx dt. \quad (23)$$

This is the analogue spacetime metric associated to the EC described by Eq. (20), which formalizes the intuition. Importantly, Eq. (23) describes an event horizon at $|\kappa| = 1$ which coincides with when the EC overtilts, as one would expect from an analogue metric. This metric has the same form as the one describing the spacetime of a radially infalling observer in the vicinity of a Schwarzschild black hole in Painlevé-Gullstrand coordinates [49]

$$ds^2 = - \left(1 - \frac{2M_0}{r}\right) dT^2 + 2\sqrt{\frac{2M_0}{r}} dr dT + dr^2, \quad (24)$$

where M_0 is the mass of the black hole, r the radial coordinate and T the Painlevé time. Considering Eq. (23) in a slice of constant y , and making the identifications $x := r$, $t := T$ and $\kappa := \sqrt{\frac{2M_0}{r}}$, the two metrics indeed coincide.

We need to comment on two caveats before moving on. First, the metrics Eqs. (23) and (24) are equal if and only if $dy = 0$, i.e., in a slice of constant y . For the analysis in the rest of this work, assuming this amounts to no loss of generality, which will become clear in Sec. IV. Second, the tilting parameter is promoted to a function with explicit spatial dependence $\kappa = \kappa(r)$, which in principle gives commutator contributions of the form $[H, \kappa(r)] \propto \frac{\partial \kappa(r)}{\partial r}$ to the eigenvalues of the Hamiltonian in Eq. (18). In the following, we ignore those contributions, and provide a rigorous discussion on the consequences of this assumption in Sec. VI.

Having formalized the analogy between ECs of NH systems and gravitational light cones, we now turn to investigate connections between physical properties between the two.

Recalling the motivation to extend already existing analogies to include NH systems, we are primarily interested in a relation between Hawking radiation from the analogue black hole and dissipation in the corresponding NH Hamiltonian.

IV. SPONTANEOUS PARTICLE EMISSION FROM QUANTUM TUNNELING

The first order contribution to Hawking radiation comes from light-like particles and antiparticles tunneling out from or into the interior of the black hole respectively, while the contribution from massive modes constitute higher-order corrections [50]. This leading contribution can be computed using the quantum tunneling method, which was first shown by Parikh and Wilczek [51]. The technique is applied in the semiclassical limit, i.e., when the mass of the black hole is very large, corresponding to $M_0 \gg 1$ in our system of units. For such black holes, the evaporation is slow enough to neglect backreaction effects from the radiation on the metric. In this section and as anticipated before, we apply the tunneling technique to our particular model, i.e., the analogue metric derived in Eq. (23). We show that there is a non-trivial contribution to the quantum tunneling process that can be interpreted as artificial spontaneous Hawking radiation. Consistently, we restrict the calculation to the region in momentum space constituting the EC in analogy to massless particles propagating along the light cone. To this end, we need to identify the possible particle and antiparticle channels contributing to the total radiation process.

A. Identifying Particle and Antiparticle Channels

When using the quantum tunneling method, the total spontaneous emission is given by the sum of two processes: a particle tunneling out from the interior of the black hole, and an antiparticle tunneling into the interior of the black hole. The quantity of interest, describing classically forbidden trajectories, is the imaginary part of the action of a pair of light-like particle and antiparticle [51]. We consider the region in momentum space corresponding to the EC [Eq. (20)] and since the spatial dependence imposed is taken to be in the x -coordinate, we solve Eq. (20) for k_x . Recalling the identification $x := r$, we get

$$k_r^\pm = -\frac{\sqrt{2M_0 r} k_z}{r - 2M_0} \pm \sqrt{\frac{r^2 k_z^2}{(r - 2M_0)^2} - \frac{r k_y^2}{r - 2M_0}}. \quad (25)$$

Since the quantum tunneling takes place close to the horizon $r = 2M_0$, we need not to worry about Eq. (25) taking complex values.

To determine which solution corresponds to particles and antiparticles respectively, we investigate the behavior of Eq. (25) when $r \rightarrow 2M_0$. The dominant term is the singular term in the Laurent expansion of Eq. (25),

$$k_r^\pm = \frac{-2M_0 k_z \pm r |k_z|}{r - 2M_0} + \mathcal{O}(r - 2M_0)^0. \quad (26)$$

Explicitly, we find

$$\lim_{r \rightarrow 2M_0^-} k_r^- = \begin{cases} +\infty, & k_z > 0, \\ 0, & k_z \leq 0, \end{cases} \quad (27)$$

indicating that k_r^- is the momentum of a *particle* trying to escape from the black hole. Analogously, k_r^+ describes the momentum of an *antiparticle* trying to fall into the black hole,

$$\lim_{r \rightarrow 2M_0^+} k_r^+ = \begin{cases} 0, & k_z > 0, \\ +\infty, & k_z \leq 0. \end{cases} \quad (28)$$

The singularities indicate that these processes are classically forbidden, and hence quantum tunneling is required to cross the horizon.

B. Quantum Tunneling

The action of the analogue radially infalling shell of energy reads

$$I = \int k_r dr, \quad (29)$$

which we want to evaluate on the EC. Hence, the action on the EC is given by

$$I = \int dr \times \left[-\frac{\sqrt{2M_0 r} k_z}{r - 2M_0} \pm \sqrt{\frac{r^2 k_z^2}{(r - 2M_0)^2} - \frac{r k_y^2}{r - 2M_0}} \right], \quad (30)$$

where an implicit sum over the two channels k_r^\pm is assumed. From Section IV A, we know that these solutions correspond to the momentum of a particle (−) and antiparticle (+), respectively. For the momentum of a particle, we consider a spontaneous radiation process in which a positive energy ω is assumed to radiate out from the interior of the black hole such that the mass of the black hole changes from M_0 to $M_0 - \omega$. Thus, the particle contribution to the action reads,

$$I_P = \int_{2M_0}^{2(M_0 - \omega)} dr \times \left[-\frac{\sqrt{2M_0 r} k_z}{r - 2M_0} - \sqrt{\frac{r^2 k_z^2}{(r - 2M_0)^2} - \frac{r k_y^2}{r - 2M_0}} \right]. \quad (31)$$

The antiparticle case, on the other hand, can be interpreted as a particle propagating backwards in time with a negative energy ω' tunneling inwards such that the mass changes from M_0 to $M_0 + \omega'$. We may thus consider the time-reversed process of a particle with negative energy tunneling into the black hole. A time-reversal transformation sends k_i to $-k_i$, and the contribution to the action from the antiparticle channel is therefore

$$I_{AP} = \int_{2M_0}^{2(M_0 + \omega')} dr \times \left[\frac{\sqrt{2M_0 r} k_z}{r - 2M_0} + \sqrt{\frac{r^2 k_z^2}{(r - 2M_0)^2} - \frac{r k_y^2}{r - 2M_0}} \right]. \quad (32)$$

The full action of the system is then given by

$$I = I_P + I_{AP}. \quad (33)$$

Now, we expand the integrand around the horizon, $r = 2M_0$, and consider the contribution from the singular terms in the Laurent series. After shifting the integration variable, we get

$$- \int_0^{-2\omega} \frac{4M_0 |k_z|}{r'} dr' + \int_0^{2\omega'} \frac{4M_0 |k_z|}{r'} dr'. \quad (34)$$

To regularize these integrals we use the Feynman $i\epsilon$ prescription as in Ref. 51. The positive energy ω is sent to $\omega - i\epsilon$, and hence $r' \rightarrow r' - i\epsilon$ in the first integral, while the negative energy ω' is sent to $\omega' + i\epsilon$ and $r' \rightarrow r' + i\epsilon$ in the second integral. The singular terms then read

$$4M_0 |k_z| \lim_{\epsilon \rightarrow 0} \left(\int_0^{2\omega'} \frac{dr'}{r' + i\epsilon} - \int_0^{-2\omega} \frac{dr'}{r' - i\epsilon} \right) = 4M_0 |k_z| \lim_{\epsilon \rightarrow 0} \int_{-2\omega}^{+2\omega} \frac{dr'}{r' - i\epsilon}, \quad (35)$$

where we in the last step used that $\omega = -\omega'$. Remarkably, all the non-singular terms in the Laurent series of I_P exactly cancel those in the Laurent series of I_{AP} . As we hinted on in Sec. III B, the imaginary part of the action is independent of k_y , which justifies setting $dy = 0$ in the metric [Eq. (23)], identifying the initial NH band structure to the light cone of a radially infalling observer in the vicinity of an artificial (3 + 1)-dimensional Schwarzschild black hole in Painlevé-Gullstrand coordinates.

Since the only contribution to the action comes from Eq. (35), it can be evaluated by dividing the contour of integration into two pieces,

$$I = 4M_0 |k_z| \lim_{\epsilon \rightarrow 0} \int_{-2\omega}^{2\omega} \frac{dr'}{r' - i\epsilon} = 4M_0 |k_z| \left(\text{P.V.} \int_{-2\omega}^{2\omega} \frac{dr'}{r'} + i\pi \int_{-2\omega}^{2\omega} \delta(r') dr' \right) = 4\pi i M_0 |k_z|, \quad (36)$$

giving the imaginary part

$$\text{Im}(I) = 4\pi M_0 |k_z|. \quad (37)$$

This indicates that there is indeed a non-vanishing contribution to the classically forbidden imaginary part of the action, and that quantum mechanical effects, such as tunneling, can take place. The probability of a tunneling event can be estimated by the semi-classical emission rate,

$$\Gamma \sim \exp(-8\pi M_0 |k_z|). \quad (38)$$

Recalling that $M_0 \gg 1$, Γ decays fast with increasing $|k_z|$, which means that a tunneling process is not likely unless $|k_z|$ is small, which we discuss in the following section.

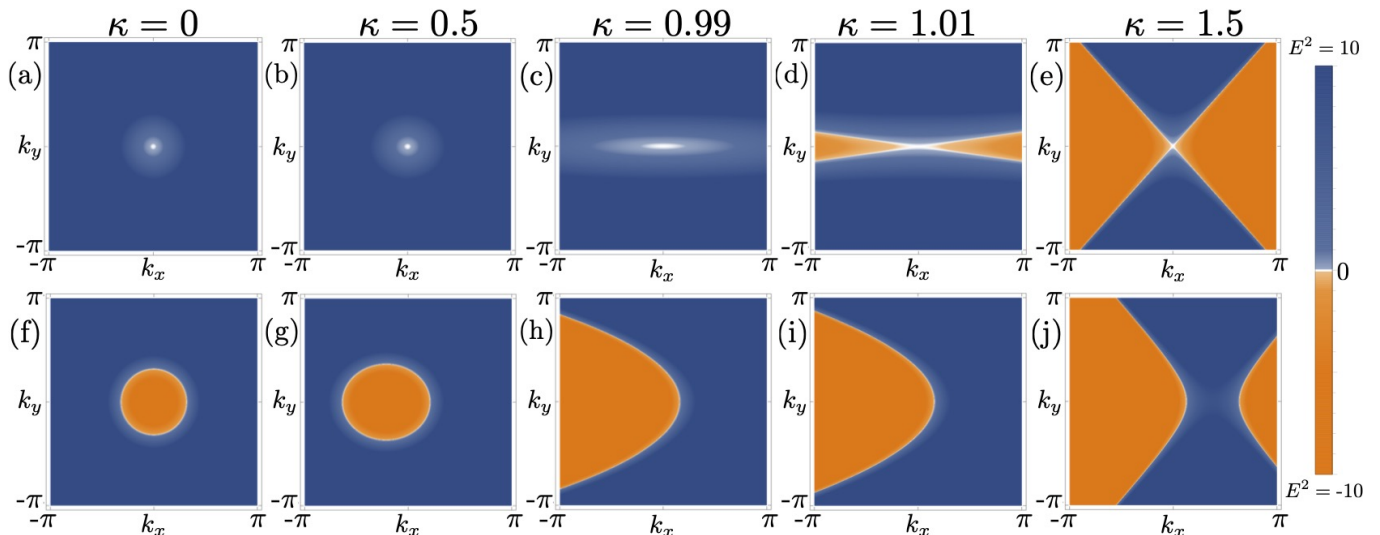


Figure 2. (a)-(e) Bulk Fermi states of the model given by Eq. (18) at $k_z = 0$ for different values of κ . For $\kappa < 1$, the bulk Fermi states are point-like, but as soon as the EC is overtilted, $\kappa > 1$, they form 2D surfaces. This indicates that at $k_z = 0$, there is no dissipative behavior unless $\kappa > 1$. This is due to the formation of a particle-antiparticle pair close to the critical point ($\kappa = 1$). To contrast this, bulk Fermi states of the same model, but at $k_z = \frac{\pi}{2}$, are displayed in (f)-(j), for the same values of κ . For finite k_z , bulk Fermi states are present for all κ , which makes the transition between the regions less clear.

V. INTERPRETATION OF PARTICLE EMISSION AS DISSIPATION

In this section we relate the spontaneous particle emission to the appearance of bulk Fermi states (BFSs) in the initial Hamiltonian (18). This means that we are able to explicitly quantify the dissipation of the NH Hamiltonian in terms of artificial Hawking radiation. Naturally, such a quantification is not possible for Hermitian band structures.

A. Bulk Fermi States and Dissipation

$$\text{Re}(E) = 0 \Rightarrow \text{Im}(E^2) = 0, \quad \text{Re}(E^2) \leq 0. \quad (39)$$

Using the Hamiltonian Eq. (18), such dissipative states correspond to

$$k_x^2 + k_y^2 - (k_z - \kappa k_x)^2 \leq 0. \quad (40)$$

Let us consider Eq. (40) for constant slices of k_z . In Figs. 2 (a)-(e), the BFSs at $k_z = 0$ are displayed for different values of κ . Notably, the BFSs appear when $\kappa > 1$, indicating that dissipative features are present when the EC overtilts. Recalling the expression for the semi-classical emission rate, Eq. (38), we note that we can regard the dissipation at $k_z = 0$ as spontaneous tunneling of light-like particles, which is the leading order contribution to Hawking radiation. We further note that the Hamiltonian Eq. (18) is dissipative also for finite k_z , which is indicated by the existence of BFSs for any value of κ when k_z is non-zero, cf. Figs. 2 (f)-(j). This region is not covered by the quantification in terms of spontaneous

emission of light-like particles, cf. Eq. (38) for $M_0 \gg 1$. An interpretation in terms of black-hole physics in this region of momentum space is beyond the scope of this project and hence left as an open question.

B. Artificial Hawking Radiation in Tight-Binding Models

A potential obstacle of the reasoning applied in Sec. V A is that the BFSs appearing when $\kappa > 1$ for $k_z = 0$ immediately become infinite. This is a direct consequence of Eq. (18) being linear in the momentum components. One way to resolve this is to consider a tight-binding model whose linearized version corresponds to Eq. (18), e.g.,

$$H_{\text{TB}} = \sin k_x \sigma^x + \sin k_y \sigma^y + i(\sin k_z - \kappa \sin k_x) \sigma^z. \quad (41)$$

Interestingly, the BFSs of this particular model, at $k_z = 0$, are also absent when $\kappa < 1$, cf. Figs. 3 (a)-(c), and they appear as soon $\kappa > 1$, cf. Figs. 3 (d)-(e). This means that the dissipation of the Hamiltonian Eq. (41) at $k_z = 0$ is also explicitly quantified as artificial Hawking radiation, by the reasoning in Sec. IV. At $k_z = \frac{\pi}{2}$, the BFSs appear rather different than in the linearized model, in particular away from $(k_x, k_y) = (0, 0)$, which is indeed expected, see Figs. 3 (f)-(j). Thus, just as in the linearized model, the dissipation at finite k_z is not quantified as tunneling of light-like particles. Furthermore, for finite k_z there is no clear transition when the EC is overtilted, which can be seen by comparing Figs. 3 (h) and (i), indicating that the interesting change of behavior occurs at $k_z = 0$.

The fact that the tight-binding model in Eq. (41) requires only nearest-neighbor hopping opens the door to possible realizations of systems with ECs in various experimental setups.

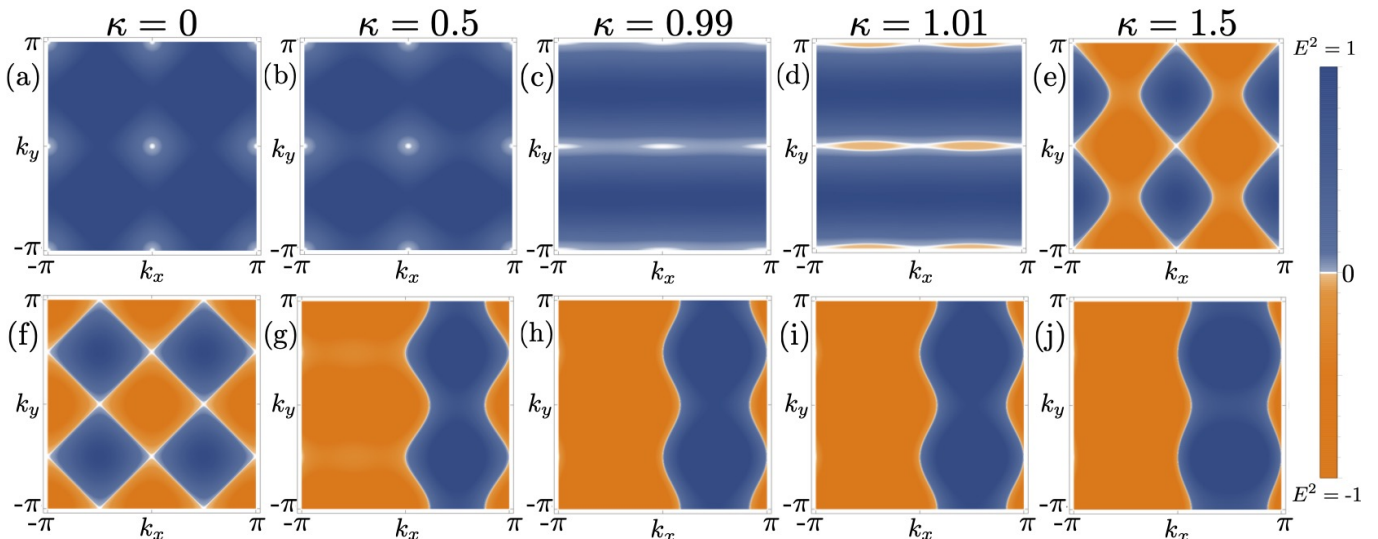


Figure 3. (a)-(e) Bulk Fermi states of the model given by Eq. (41) at $k_z = 0$ for different values of κ . As in Fig. 2, the bulk Fermi states are point-like when $\kappa < 1$, but attain the form of 2D surfaces when the EC is overtilted. In the regime where the linear approximation is motivated, this can be interpreted as a spontaneous creation and emission of a particle-antiparticle pair around $\kappa = 1$. For finite k_z , illustrated for $k_z = \frac{\pi}{2}$ in (f)-(j), there is no clear difference between the cases when $\kappa < 1$ and $\kappa > 1$, which indicates $k_z = 0$ is indeed the point of interest.

Potential candidates include disordered and non-equilibrium systems, but also photonic lattices [38, 39], which have recently been used to realize dissipative systems of more complicated nature [37]. Since Hawking radiation in stationary Schwarzschild black holes appears as quantum fluctuations of an otherwise classical system, it would be intriguing to investigate photonic crystals and see if similar phenomena related to spontaneous emission of particles can be observed. Suggestive methods include ARPES measurements to image the BFSs at $k_z = 0$ and around $\kappa = 1$. Tuning κ to vary slowly with respect to space around $\kappa = 1$, the transition illustrated in Figs. 3 (c) and (d) should be observable.

VI. DISCUSSION AND OUTLOOK

One of the first assumptions we made when modelling the artificial Schwarzschild event horizon, was to neglect the commutator contributions occurring when the tilting parameter κ was assigned an explicit spatial dependence. Let us now investigate what this means. The neglected commutators turn out to be proportional to a more simple commutator. This can be seen by explicitly plugging in the expression for the Hamiltonian from Eq. (18) and recalling the identification $x := r$. This yields

$$[H, \kappa(r)] \propto [k_r, \kappa(r)], \quad (42)$$

and

$$[H, k_r] \propto [k_r, \kappa(r)], \quad (43)$$

and evaluates to

$$[k_r, \kappa(r)] \propto \frac{\partial \kappa(r)}{\partial r} \propto \frac{M_0}{r^2 \sqrt{\frac{2M_0}{r}}}. \quad (44)$$

When moving away from the horizon this goes as $r^{-3/2}$, and thus decays for increasing r . However, the quantum tunneling occurs close to the horizon, and therefore, we also have to make sure that it is well motivated to neglect the commutator there. At the horizon, the commutator is

$$[k_r, \kappa(r)]|_{r=2M_0} \propto M_0^{-1}. \quad (45)$$

As we assumed $M_0 \gg 1$, this contribution indeed disappears.

We note that the current study exclusively deals with stationary phenomena, both in terms of black holes and in terms of topological phases. Previous works in the Hermitian realm have used a Lagrangian formalism to study the time-dependence of solutions to the Euler-Lagrange equations [24]. These are shown to not result in any radiative behavior over time, indicating that Hermitian systems model artificial black holes in equilibrium. Unfortunately, similar studies cannot be extended in a straightforward manner to NH systems, since the conventional stationary action principle is not applicable. The action corresponding to a NH Hamiltonian necessarily becomes complex, and hence one would have to choose whether to minimize, e.g., its real part, imaginary part or absolute value. Instead, we suggest that time dependence can be introduced differently into NH Hamiltonians through dissipation. Including time as an explicit variable in the Hamiltonian requires a more thorough relation to the gravitational side [19, 23]. In principle, in such an analogy, the time-dependent dissipation could be used to mimic black hole evaporation. The latter remains an open question in the current setup.

We also note that the creation (and emission) of the particle-antiparticle pair occurs exactly on the EC, where \mathcal{PT} symmetry is spontaneously broken. This has, to our knowledge, not been observed before and should be investigated in other setups to see whether or not it is a generic feature. However, this is beyond the scope of this article.

In recent works, the importance of additional bands in similar NH models has been studied [52, 53]. In particular, the appearance of higher order EPs is investigated. To this point, we note that considering additional bands, the ECs of order two can be accompanied by third order exceptional lines and fourth order EPs in 3D \mathcal{PT} -symmetric systems. The impact of the higher order exceptional structure is something that we find interesting, but nothing that we intend to investigate at this point. Here we assume the additional bands to be located far away from the ones considered in this work, and leave further investigation for future studies.

VII. CONCLUSION

In this work, we studied analogies between the band structures of \mathcal{PT} -symmetric NH two-band models and curved spacetime geometries. As an extension of the previous analogies mapping Weyl cones to light cones, we found a relation between the \mathcal{PT} symmetry protected cone of EPs, dubbed the EC, and the radially infalling observer's light cone in the vicinity of a 4D stationary Schwarzschild black hole. By applying the quantum tunneling method for light-like modes, corresponding to momenta located on the EC, we showed that the leading order contribution of (artificial) Hawking radiation was finite/non-trivial. This spontaneous emission was then interpreted in terms of the existence of dissipative BFS in continuous and lattice models.

We thus extended the previously known Hermitian rela-

tion to artificial light cones to include NH systems. This allowed for the interpretation of spontaneous Hawking radiation as dissipative features, which was not possible for Hermitian systems. Interestingly, recent studies show that NH systems can be related to general features of quantum gravity [54, 55], indicating further interpretations and applications of non-Hermiticity in the study of the nature of spacetime. Hopefully, further studies will sharpen and clarify the analogy between dissipative NH systems and black hole physics.

ACKNOWLEDGEMENTS

We would like to thank Emil J. Bergholtz, Johan Carlström and Watse Sybesma for useful discussions. Special thanks to Thors Hans Hansson, Igor Pikovski, Bo Sundborg and Lårus Thorlacius for useful comments on the manuscript. M.S. is supported by the Swedish Research Council (VR) and the Wallenberg Academy Fellows program of the Knut and Alice Wallenberg Foundation. L.R. is supported by the Knut and Alice Wallenberg foundation under grant no. 2017.0157. F.K.K. is supported by the Max Planck Institute of Quantum Optics (MPQ) and Max-Planck-Harvard Research Center for Quantum Optics (MPHQ). The work was finished while JLA and LR were participating in a mathematical physics conference, organized by Uppsala University and funded by the Göran Gustafsson foundation, whose stimulating environment is also acknowledged.

-
- [1] K.v. Klitzing, G. Dorda, and M. Pepper, *New Method for High-Accuracy Determination of the Fine-Structure Constant Based on Quantized Hall Resistance*, Phys. Rev. Lett. **45**, 494 (1980), doi:10.1103/PhysRevLett.45.494.
- [2] M.Z. Hasan and C.L. Kane, *Colloquium: Topological insulators*, Rev. Mod. Phys. **82**, 3045 (2010), doi:10.1103/RevModPhys.82.3045.
- [3] X.-L. Qi and S.-C. Zhang, *Topological insulators and superconductors*, Rev. Mod. Phys. **83**, 1057 (2011), doi:10.1103/RevModPhys.83.1057.
- [4] M.O. Goerbig, *Electronic properties of graphene in strong magnetic field*, Rev. Mod. Phys. **83**, 1193 (2011), doi:10.1103/RevModPhys.83.1193.
- [5] N.P. Armitage, E.J. Mele, and A. Vishwanath, *Weyl and Dirac semimetals in three-dimensional solids*, Rev. Mod. Phys. **90**, 015001 (2018), doi:10.1103/RevModPhys.90.015001.
- [6] J.C. Budich and B. Trauzettel, *From the adiabatic theorem of quantum mechanics to topological states of matter*, physica status solidi (RRL) **7**, 109 (2013), doi:10.1002/pssr.201206416.
- [7] H. Weyl, *Elektron und Gravitation. I*, Z. Physik **56**, 330 (1929), doi:10.1007/BF01339504.
- [8] S.-Y. Xu, I. Belopolski, N. Alidoust, M. Neupane, G. Bian, C. Zhang, R. Sankar, G. Chang, Z. Yuan, C.-C. Lee, S.-M. Huang, H. Zheng, J. Ma, D.S. Sanchez, B. Wang, A. Bansil, F. Chou, P.P. Shibayev, H. Lin, S. Jia, and M.Z. Hasan, *Discovery of a Weyl fermion semimetal and topological Fermi arcs*, Science **349**, 613 (2015), doi:10.1126/science.aaa9297.
- [9] B.Q. Lv, H.M. Weng, B.B. Fu, X.P. Wang, H. Miao, J. Ma, P. Richard, X.C. Huang, L.X. Zhao, G.F. Chen, Z. Fang, X. Dai, T. Qian, and H. Ding, *Experimental Discovery of Weyl Semimetal TaAs*, Phys. Rev. X **5**, 031013 (2015), doi:10.1103/PhysRevX.5.031013.
- [10] L. Lu, Z. Wang, D. Ye, L. Ran, L. Fu, J. D. Joannopoulos, and M. Soljacic, *Experimental observation of Weyl points*, Science **349**, 6248, 622-624 (2015), doi:10.1126/science.aaa9273.
- [11] H. B. Nielsen and M. Ninomiya, *The Adler-Bell-Jackiw anomaly and Weyl fermions in a crystal*, Phys. Lett. B **130**, 389 – 396 (1983), doi:10.1016/0370-2693(83)91529-0.
- [12] K. Fukushima, D. E. Kharzeev, and H. J. Warringa, *Chiral magnetic effect*, Phys. Rev. D **78**, 074033 (2008), doi:10.1103/PhysRevD.78.074033.
- [13] A. A. Zyuzin and A. A. Burkov, *Topological response in weyl semimetals and the chiral anomaly*, Phys. Rev. B **86**, 115133 (2012), doi:10.1103/PhysRevB.86.115133.

- [14] M. M. Vazifeh and M. Franz, *Electromagnetic Response of Weyl Semimetals*, Phys. Rev. Lett. **111**, 027201 (2013), doi:10.1103/PhysRevLett.111.027201.
- [15] W. G. Unruh, *Experimental black-hole evaporation?*, Phys. Rev. Lett. **46**, 1351–1353 (1981).
- [16] C. Barceló, S. Liberati, and M. Visser, *Analogue gravity*, Living Rev. Relativity **14**, 3 (2011).
- [17] C. Beenakker, Commentary at the Journal Club for Condensed Matter Physics (2015), <https://www.condmatclub.org/?p=2644>.
- [18] G.E. Volovik, *The Universe in a Helium Droplet* (Clarendon, Oxford, 2003), doi: 10.1093/acprof:oso/9780199564842.001.0001.
- [19] P. Hořava, *Stability of Fermi Surfaces and K-Theory*, Phys. Rev. Lett. **95**, 016405 (2005), doi:10.1103/PhysRevLett.95.016405.
- [20] G.E. Volovik, and K. Zhang, *Lifshitz Transitions, Type-II Dirac and Weyl Fermions, Event Horizon and All That*, J. Low Temp. Phys. **189**, (2017), doi:10.1007/s10909-017-1817-8.
- [21] M.A. Zubkov, *Analogies between the Black Hole Interior and the Type II Weyl Semimetals*, Universe **2018**, **4** (12), **135**, doi:10.3390/universe4120135.
- [22] H. Liu, J.-T. Sun, H. Huang, F. Liu, and S. Meng, *Fermionic analogue of black hole radiation with a super high Hawking temperature*, arXiv:1809.00479.
- [23] G.E. Volovik, and M.A. Zubkov *Emergent Weyl spinors in multi-fermion systems*, Nuclear Physics, B **881** (2014), doi: 10.1016/j.nuclphysb.2014.02.018.
- [24] Y. Kedem, E.J. Bergholtz, and F. Wilczek *Black and White Holes at Material Junctions*, Phys. Rev. Research **2**, 043285 (2020), doi:10.1103/PhysRevResearch.2.043285.
- [25] S.W. Hawking, *Particle creation by black holes*, Comm. Math. Phys. **43**, 199 (1975), doi:10.1007/BF02345020.
- [26] E.J. Bergholtz, J.C. Budich, and F.K. Kunst, *Exceptional topology of non-Hermitian systems*, Rev. Mod. Phys. **93**, 015995 (2021), doi:10.1103/RevModPhys.93.015995.
- [27] D.C. Brody, *Biorthogonal quantum mechanics*, Journal of Physics A: Math. Theor. **47** 034305 (2014), doi:10.1088/1751-8113/47/3/035305.
- [28] M. Berry, *Physics of Nonhermitian Degeneracies*, Czechoslovak Journal of Physics **54**, 1039 (2004), doi: 10.1023/B:CJOP.0000044002.05657.04.
- [29] J. Carlström and E.J. Bergholtz, *Exceptional links and twisted Fermi ribbons in non-Hermitian systems*, Phys. Rev. A **98**, 042114 (2018), doi:10.1103/PhysRevA.98.042114.
- [30] R.A. Molina and J. Gonzalez, *Surface and 3D Quantum Hall Effects from Engineering of Exceptional Points in Nodal-Line Semimetals*, Phys. Rev. Lett. **120**, 146601 (2018), doi:10.1103/PhysRevLett.120.146601.
- [31] K. Moors, A.A. Zyuzin, A.Y. Zyuzin, R.P. Tiwari and T.L. Schmidt, *Disorder-driven exceptional lines and Fermi ribbons in tilted nodal-line semimetals*, Phys. Rev. B **99**, 041116(R) (2019), doi:10.1103/PhysRevB.99.041116.
- [32] V. Kozii and L. Fu, *Non-Hermitian Topological Theory of Finite-Lifetime Quasiparticles: Prediction of Bulk Fermi Arc Due to Exceptional Point*, arXiv:1708.05841 (2017).
- [33] J. Carlström, M. Stålhammar, J.C. Budich, and E.J. Bergholtz, *Knotted Non-Hermitian Metals*, Phys. Rev. B **99**, 161115(R) (2019), doi:10.1103/PhysRevB.99.161115.
- [34] C.H. Lee, G. Li, Y. Liu, T. Tai, R. Thomale, and X. Zhuang, *Tidal surface states as fingerprints of non-Hermitian nodal knot metals*, Communications Physics **4**, 47 (2021), doi: 10.1038/s42005-021-00535-1.
- [35] M. Stålhammar, L. Rødland, G. Arone, J.C. Budich and E.J. Bergholtz, *Hyperbolic nodal band structures and knot invariants*, SciPost Physics **7**, 019 (2019), doi: 10.21468/SciPostPhys.7.2.019.
- [36] J.C. Budich, J. Carlström, F.K. Kunst, and E.J. Bergholtz, *Symmetry-protected nodal phases in non-Hermitian systems*, Phys. Rev. B **99**, 041406(R), doi: 10.1103/PhysRevB.99.041406.
- [37] K. Wang, L. Xiao, J.C. Budich, W.Yi, and P. Xue, *em Simulating Exceptional Non-Hermitian Metals with Single-Photon Interferometry*, arXiv:2011.01884.
- [38] L Lu, J.D. Joannopoulos, and M. Soljačić, *Topological Photonics*, Nature Photonics **8** (2014), doi:10.1038/nphoton.2014.248.
- [39] B.A. Bell, K. Wang, A.S. Solntsev, D.N. Neshev, A.A. Sukhorukov, and B.J. Eggleton, *Spectral photonic lattices with complex long-range coupling*, Optica **4**, 11 (2017), doi:10.1364/OPTICA.4.001433.
- [40] D. Bernard and A. LeClair, "A classification of non- hermitian random matrices", in *Statistical Field Theories*, edited by A. Cappelli and G. Mussardo (Springer Netherlands, Dordrecht, 2002) pp. 207-214.
- [41] D. Bernard and A. LeClair, *A Classification of Non- Hermitian Random Matrices*, arXiv:0110649.
- [42] C. Herring, *Accidental Degeneracy in the Energy Bands of Crystals*, Phys. Rev. **52** 365 (1937), doi: 10.1103/PhysRev.52.365.
- [43] M. Ezawa, *Topological semimetals carrying arbitrary Hopf numbers: Fermi surface topologies of a Hopf link, Solomon's knot, trefoil knot, and other linked nodal varieties*, Phys. Rev. B **96**, 041202(R) (2017), doi:10.1103/PhysRevB.96.041202.
- [44] Z. Yan, R. Bi, H. Shen, L. Lu, S.-C. Zhang, and Z. Wang, *Nodal-link semimetals*, Phys. Rev. B **96**, 041103(R) (2017), doi:10.1103/PhysRevB.96.041103.

- [45] G. Chang, S.-Y. Xu, X. Zhou, S.-M. Huang, B. Singh, B. Wang, I. Belopolski, J. Yin, S. Zhang, A. Bansil, H. Lin, and M.Z. Hasan, *Topological Hopf and Chain Link Semimetal States and Their Application to Co_2MnGa* , Phys. Rev. Lett. **119**, 156401, doi:10.1103/PhysRevLett.119.156401.
- [46] L. Li, C.H. Lee, and J. Gong, *Realistic Floquet Semimetal with Exotic Topological Linkages between Arbitrarily Many Nodal Loops*, Phys. Rev. Lett. **121**, 036401, doi:10.1103/PhysRevLett.121.036401.
- [47] R. Bi, Z. Yan, L. Lu and Z. Wang, *Nodal-knot semimetals*, Phys. Rev. B **96**, 201305 (2017), doi:10.1103/PhysRevB.96.201305.
- [48] S. M. Carroll, *Spacetime and Geometry: An Introduction to General Relativity*, Addison-Wesley (2003), ISBN-13 978-0805387322.
- [49] P. Painlevé, *La mécanique classique et la théorie de la relativité*, C. R. Acad. Sci. (Paris) **173**, (1921).
- [50] A. Coutant, A. Fabbri, R. Parentani, R. Balbinot, and P.R. Anderson, *Hawking radiation of massive modes and undulations*, Phys. Rev. D **86** 064022 (2012), doi:10.1103/PhysRevD.86.064022.
- [51] M.K. Parikh and F. Wilczek, *Hawking Radiation as Tunneling*, Phys. Rev. Lett. **85**, 5042 (2000), doi:10.1103/PhysRevLett.85.5042.
- [52] I. Mandal, and E.J. Bergholtz, *Symmetry and Higher-Order Exceptional Points*, arXiv:2103.15729.
- [53] P. Delplace, T. Yoshida, and Y. Hatsugai, *Symmetry-protected higher-order exceptional points and their topological characterization*, arXiv:2103.08232.
- [54] C. Lv, R. Zhang and Q. Zhou, *Curving the space by non-Hermiticity*, arXiv:2106.02477.
- [55] L. M. Lawson, *Minimal and maximal lengths from position-dependent non-commutativity*, arXiv:2012.06906.

Appendix A: Cones of Exceptional Points in \mathcal{PT} -symmetric Systems and Their Analogue Event Horizons

In this Appendix, we show that any 3D NH \mathcal{PT} -symmetric two-band model linear in momentum host cones of EPs, which can be mapped to a curved spacetime metric. Since we are only interested in the EPs, and not the eigenvalues themselves, we can set the term proportional to the identity matrix to 0. Generally, in an appropriate choice of coordinates, the Hamiltonian attains the form

$$H = (a_x k_x + a_y k_y + a_0) \sigma^x + (b_x k_x + b_y k_y + b_0) \sigma^y + i (c_x k_x + c_y k_y + c_z k_z + c_0) \sigma^z, \quad (\text{A1})$$

with all parameters being real. We note that the constant terms a_0 , b_0 and c_0 can be set to 0, since they can be removed by shifting the momentum components. Explicitly, the corresponding EPs are given by

$$(a_x^2 + b_x^2 - c_x^2) k_x^2 + (a_y^2 + b_y^2 - c_y^2) k_y^2 - c_z^2 k_z^2 + 2k_x k_y (a_x a_y + b_x b_y - c_x c_y) - 2c_y c_z k_y k_z - 2c_x c_z k_x k_z = 0, \quad (\text{A2})$$

and solving for k_z yields,

$$k_z = -\frac{1}{c_z} (c_x k_x + c_y k_y) \pm \sqrt{(a_x k_x + a_y k_y)^2 + (b_x k_x + b_y k_y)^2}. \quad (\text{A3})$$

with $c_z \neq 0$. As in the simple example dealt with in the main text, k_z can be thought of as the eigenvalue of some Dirac-like operator, in this case, e.g.,

$$\hat{k}_z = -\frac{1}{c_z} (c_x k_x + c_y k_y) \sigma^0 + (a_x k_x + a_y k_y) \sigma^x + (b_x k_x + b_y k_y) \sigma^y, \quad (\text{A4})$$

whose eigenvalues form a cone. It should be stressed that adding a term proportional to σ^z Eq. (A4) would correspond to adding an equivalent term to the initial Hamiltonian Eq. (A1), which would break the implemented \mathcal{PT} -symmetry. Hence, such terms are forbidden, and we note more accurately that k_z can be thought of the eigenvalues of a Hermitian Dirac-operator subject to \mathcal{PT} -symmetry.

Since a Dirac-operator can be expressed in terms of vielbeins [18, 19], we can write \hat{k}_z on the form

$$\hat{k}_z = e^i_a k_i \sigma^a + e^i_0 k_i \sigma^0 \quad (\text{A5})$$

with

$$\begin{aligned} e^0_0 &= 1, & e^x_0 &= -\frac{c_x}{c_z}, & e^y_0 &= -\frac{c_y}{c_z}, & e^0_x &= 0, \\ e^0_y &= 0, & e^x_x &= a_x, & e^x_y &= b_x, & e^y_x &= a_y, & e^y_y &= b_y, \end{aligned} \quad (\text{A6})$$

from which a curved spacetime metric can be defined through $g_{\mu\nu} = e_\mu^\alpha e_\nu^\beta \eta_{\alpha\beta}$.